The Impact of Satellite-Sensed Winds on Intensity Forecasts of Tropical Cyclones

SIMON WEI-JEN CHANG[1]

JAYCOR, Alexandria, VA 22304

(Manuscript received 25 September 1980, in final form 20 November 1980)

ABSTRACT

The impact of satellite-sensed winds on the intensity forecasts of tropical cyclones is evaluated by a simulation study with an axisymmetric numerical model. The parameterized physics in the forecast model are deliberately made different from those in the model that generates the observation. Model-generated "observations" are assimilated into forecasts by 12 h dynamic initialization.

A series of 24 h forecasts with and without assimilation of satellite-sensed winds are conducted and compared with the observations. Results indicate that assimilation with marine surface (or low-level) wind alone does not improve intensity forecasts appreciably, that a strong relaxation coefficient in the initialization scheme causes model rejection of the assimilation, and that an attenuating relaxation coefficient is recommended. However, when wind observations at the outflow level are included in the assimilation, forecasts improve substantially. The best forecasts are achieved when observations over the entire lower troposphere are assimilated.

Additional experiments indicate the errors in the satellite observations contaminate the forecast. But the assimilation of inflow and outflow winds still improve the intensity forecast if the satellite observation errors are less than or about the same magnitude of those in the initial wind field.

1. Introduction

The improvement of forecast skill in tropical cyclones evident in the 1960's has not been continued in the 1970's in spite of improved technology and continuing effort. The lack of improvement has been attributed to the imperfect knowledge of the initial fields for objective models. Elsberry (1977) attributed the poor performance of his prediction model to the deficiency of the initial wind data. For the 1976 Atlantic tropical cyclone season, Hovermale and Livezey (1977) showed the errors for the 36 and 48 h track forecasts increased by approximately a factor of 3 for storms over data-void ocean regions as compared to storms near coastal stations. In addition, the theory of geostrophic adjustment requires that the mass field adjusts to the momentum field for low latitudes and tropical cyclone scales of motion (Monin and Obukhov, 1959; Washington, 1964). It is beyond doubt that wind observations are essential to tropical cyclone forecasts.

Although initial wind analyses of tropical cyclones have been improved from reconnaissance aircraft flights, the quantity and especially the aerial coverage of wind data so obtained are inadequate for numerical model initializations. Remote measurements from geostationary and orbiting satellites will be relied upon as important data sources. Rodgers *et al.* (1979) explained techniques to derive low-level and outflow-level winds for tropical cyclones by tracking clouds using successive satellite images. Their results are encouraging in spite of some difficulties such as the short lives of cloud turrets and overcast conditions near the storm centers. An experimental oceanographic satellite known as SEASAT-A during its short lifetime provided an additional data source to define large and mesoscale wind fields near tropical cyclones. A special scatterometer (SASS) flown with SEASAT-A measured the marine surface microstructures and, through appropriate algorithms, marine surface winds were inferred.

The purpose of this study is to evaluate the impact of the satellite-sensed winds on tropical cyclone intensity forecasts. As a simulation study, data generated by numerical models will be used in place of real data. The general strategy of such simulation studies follows that of Charney *et al.* (1969). First, a control integration of the numerical forecast model is performed to generate the "true" history of the atmosphere or the "observation". A series of "standard forecasts" is then generated based on different initial states. Finally, a series of forecasts with the "observations" assimilated are conducted to evaluate the impact of assimilation. For detailed reviews of such simulation studies and their general strategies, readers are referred to McPherson (1975) and Bengtsson (1975).

As a preliminary study, an axisymmetric tropical cyclone model is employed in this study; therefore only the impact on intensity can be studied. The

[1] Present affiliation: Science Applications, Inc. McLean, VA 22102.

0027-0644/81/030539-15$07.75
© 1981 American Meteorological Society

Unauthenticated | Downloaded 06/24/24 04:14 AM UTC

TABLE 1. Vertical structure of the model.

Layer	ΔP (mb) for P_s = 1000	Undisturbed height (km) at layer center
1	0–200	18.3
2	200–300	10.6
3	300–600	6.7
4	600–800	3.0
5	800–930	1.2
6	930–1000	0.3

method of assimilation used is the dynamic initialization by relaxation (DIR) technique. To approximate the relationship between the real atmosphere and forecast models, parameterized physics in the model that generates forecasts (forecast model) are altered from those in the model that generate the observations (natural model). In the following sections, the numerical model, the experimental design and the method of assimilation will be discussed in sequence. Finally, the results, conclusions and proposed future research will be presented.

2. Numerical model

The axisymmetric tropical cyclone model used in this study is similar to the one described in Chang (1977) and Anthes and Chang (1978). The governing equations are in primitive form and are in σ ($=P/P_s$) coordinates. The explicit water vapor cycle and parameterization of cumulus convection follow Kuo (1974) and Anthes (1977). The boundary layer is contained in the lowest model layer and parameterization of various vertical fluxes is based on a generalized similarity theory in which Yamada's (1976) universal functions are used (Chang, 1981). Charnock's equation is applied to compute marine surface roughness length.

The model atmosphere is divided into six layers (Table 1). A uniform horizontal grid interval of 30 km is used from the center to a radius of 600 km. The grid interval is progressively increased by a factor of 2 outside 600 km. The leapfrog temporal integration method with the time-averaged pressure gradient force (Brown and Campana, 1978) is employed for numerical integration. The spatial finite differencing is of the second order. The mean hurricane season sounding (Sheets, 1969) is used for the initial and lateral boundary conditions. The Coriolis parameter f has the constant value 5×10^{-5} s^{-1}.

A period of 36 h of the control run during which the model tropical cyclone undergoes a rapid intensification is chosen as the "truth" or "observation" (thereafter referred to as such in this study except as stated otherwise). For convenience, −12 and 24 h are designated as the start and end of this period. We selected a period of rapid intensification for study in order to magnify errors in the forecasts.

3. Experimental design

In recent years, many simulation studies have been conducted to evaluate the impact of incomplete observation data on numerical predictions (e.g., Charney *et al.*, 1969; Kasahara and Williamson, 1972; Morel and Talagrand, 1974; Anthes, 1974; Cane *et al.*, 1979). In a similar manner, numerical integrations conducted for this study can be grouped into three components (Table 2):

1) *Nature run.* A 36 h segment of life history of tropical cyclones designated as observation as defined in Section 2.

2) *Standard forecasts.* A 36 h forecast starting from −12 and 24 h forecast starting from 0 h. The initial conditions for standard forecasts are obtained by the static, nondivergent initialization method based on the nature run.

TABLE 2. List of simulation experiments.

Components	Experiments	Total length of integration (h)	Assimilation period (h)	Observations assimilated	Relaxation coefficient
Nature	1	−12 to 24	Observation		
Forecasts	2	−12 to 24	Standard 36 h forecast		
	3	0 to 24	Standard 24 h forecast		
Forecasts with low-level wind observations assimilated	4	−12 to 24	−12 to 0	u_6, v_6*	Weak
	5	−12 to 24	−12 to 0	u_6, v_6	Strong
	6	−12 to 24	−12 to 0	u_6, v_6	Attenuating
Forecasts with low-level and higher level wind observations assimilated	7	−12 to 24	−12 to 0	v_5, u_6, v_6	Attenuating
	8	−12 to 24	−12 to 0	v_4, v_5, u_6, v_6	Attenuating
	9	−12 to 24	−12 to 0	u_2, v_2, u_6, v_6	Attenuating
Forecasts with low and outflow winds containing errors assimilated	9E	−12 to 24	−12 to 0	u_2, v_2, u_6, v_6	Attenuating
	9E2	−12 to 24	−12 to 0	u_2, v_2, u_6, v_6	Attenuating

* u, v are radial and tangential winds, respectively. Subscripts denote layers.

Unauthenticated | Downloaded 06/24/24 04:14 AM UTC

3) *Forecasts with assimilation.* 12 h preforecast integrations starting from −12 h, during which satellite-sensed winds are assimilated into the model solution followed by 24 h forecasts starting from 0 h.

A unique characteristic of previous simulation studies is that a prediction model will make an error-free forecast given error-free model-generated initial conditions (Williamson, 1973). Because this is rather unrealistic, errors of various kinds were added to the observations either in initial conditions for the forecasts, or in data for assimilation. Both random errors (e.g., Williamson and Kasahara, 1971) and bias errors (e.g., Anthes, 1974) have been introduced into the observations in previous studies. Forecast runs with initial random errors sometimes exhibit unrealistic error growth characteristics because gravity waves and model physics act to smooth them. Besides, random observational errors are not the major problem with real data, where systematic errors are known to have caused more problems (McPherson, 1975). Biased errors are generally determined subjectively and may be unwarranted and unrealistic. No error is artificially added in the initial fields for all forecast runs in our study; instead, errors in the initial wind fields are introduced by the nondivergent, gradient-balanced, static initialization procedure adopted here. Such initialization procedure is currently in use operationally. Fig. 1 shows the speed errors in the initial wind fields of forecasts at −12 h. As expected, large errors occur in the low-level and the outflow level, where divergent components of wind vectors are largest. The initial errors for forecasts initialized at 0 h have the same characteristics.

In previous simulation studies, the models which generated the forecasts were identical with the models that generated the observations (for a review see McPherson, 1975). This, of course, is very unrealistic. In reality, numerical forecasting models with finite spatial resolutions and parameterized physics cannot reproduce the atmosphere even if perfect initial conditions are obtained. To properly account for the discrepancies between real forecasting models and the atmosphere, the parameterized physics in our forecast model is deliberately altered. The parameters changed are those we feel most uncertain about in the physical parameterizations in current numerical models, namely, the effective air-sea exchange coefficients and the vertical distribution of latent heat. The effective coefficients of eddy transfers of momentum, sensible heat and latent heat in the forecast model are set at 90% of those in the nature model. The 10% error is well within the expected error in the boundary layer formulations. The vertical distribution of cumulus heating is also changed so that ~5% of the heating in the lower troposphere is shifted to the upper troposphere. The 5% difference is within the variation of the observed heating distributions. Due to these two changes, the forecasts in our study do not asymptotically approach the observations even after long integration. Because the errors in the parameterized physics in our forecast model are within the differences between the atmosphere and the current operational forecast models, the asymptotic difference between our "forecasts" and "observation" should be quite realistic.

4. Method of assimilation

The satellite-sensed data are in many occasions incomplete in that they do not contain observations of all meteorological variables simultaneously or the

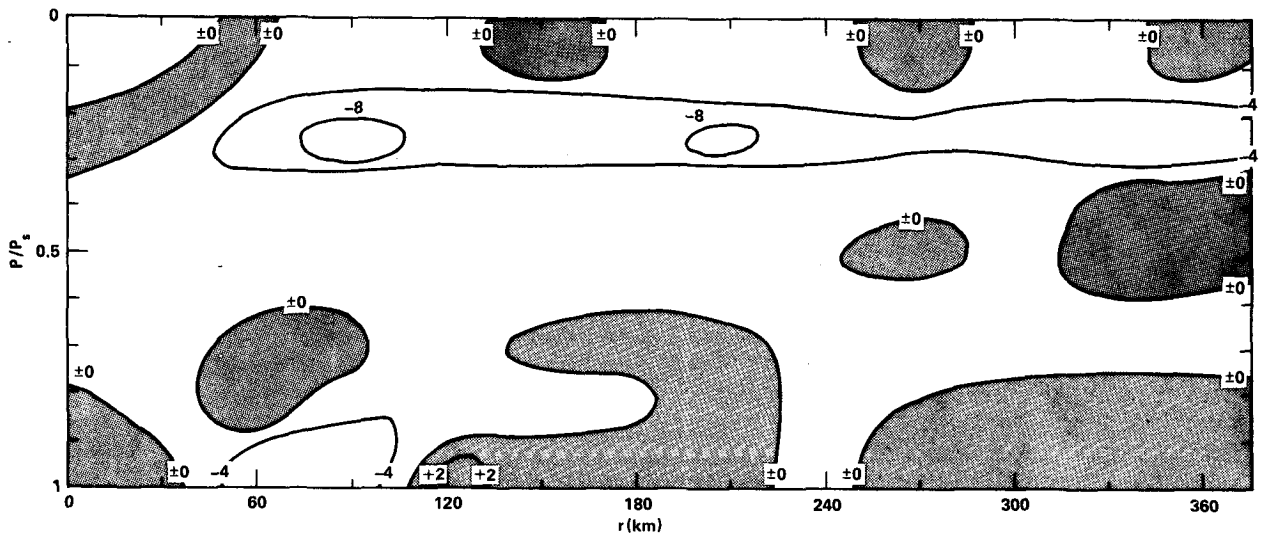

FIG. 1. Wind speed errors (m s^{-1}) in the initial ϕ condition at −12 h after a nondivergent, static initialization.

Unauthenticated | Downloaded 06/24/24 04:14 AM UTC

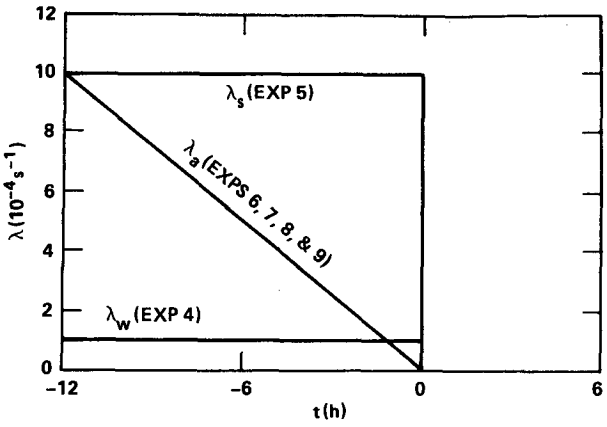

FIG. 2. The three relaxation coefficients used in DIR: λ_w for weak relaxation, λ_s for strong relaxation, and λ_a for attenuating relaxation.

observations are made at different locations and times. To incorporate such data in a dynamically consistent way into the numerical models, suitable methods of assimilation must be used. From the direct insertion method (e.g., Charney *et al.*, 1969) to the complicated variational assimilation (e.g., Sasaki, 1969), there are many methods of assimilation in existence. However, not all methods are applicable for the satellite-sensed data in question. The wind fields derived from GOES images are basically restricted to low and outflow levels in tropical cyclones (Rodgers *et al.*, 1979), and wind fields measured from SEASAT-A are at anemometer level. For such data with poor vertical resolution, a method called dynamic initialization by relaxation (DIR) is desirable.

DIR is a technique wherein the meteorological variables are relaxed (or nudged) by using the model's governing equations toward the observed values during a preforecast integration (Anthes, 1974; Hoke and Anthes, 1976). The technique has shown great promise in real data applications (Nitta and Hovermale, 1969; Davies and Turner, 1977; Hoke and Anthes, 1977). Mathematically, governing equations during the preforecast integrations are modified to

$$\frac{\partial x}{\partial t} = F(\mathbf{X},t) + \sum_{n=1}^{N} \lambda(\epsilon_n,\delta t,\delta r,\delta z)(x^0 - x), \quad (1)$$

where x is an element in the vector of variables $\mathbf{X}$, the function F contains the normal terms in governing equations, x^0 is the observation, N the number of observations, and λ the relaxation coefficient. In a full four-dimensional assimilation, λ is the function of observational error ϵ_n, the time separation of the observation δt, and the horizontal (δr) and the vertical (δz) spatial separations between observations and grid points. It should also depend on the meteorological variables.

To simplify the functional form of λ, we will use point-to-point relaxation, i.e., variables are relaxed toward observations made at the same model grid points only. This requires that observations be taken at model grid points and all observations be taken simultaneously. Note that the horizontal resolution of the satellite measurements does approach those of typical operational forecast models of tropical cyclones. With the development of suitable boundary-layer models for vertical extrapolation (Yu, 1980), the convenience of point-to-point relaxation assumed for convenience in this study is nearly available in operational forecasting. The time lag of measurements over the domain of tropical cyclones within one satellite revolution is negligibly short as compared to the 12 h preforecast integration. We take note that the swath width of orbiting satellites nevertheless may not be large enough to cover the entire tropical cyclone.

The satellite-sensed winds are not free of errors. Rodgers *et al.* (1979) estimated the mean speed errors in their derived winds to be 2.5 m s^{-1} relative to aircraft measurements. There are conflicting reports on the errors of SEASAT measurements (Black, 1979; Jones and Pierson, 1978), but, in general, the errors of satellite-sensed winds are smaller than those introduced by the objective analyses over the oceans (Cardone *et al.*, 1976). The contribution of satellite measurements is not in the general error reduction but in the filling of data-void areas (Ghil *et al.*, 1979). For a clear demonstration of the impact in assimilating winds at different levels, it is justifiable in Exps. 4–9 to assume that the satellite observations are error-free in comparison to the initial and model errors. However, errors of different magnitudes are added to the satellite-sensed wind in Exps. 9E and 9E2 to evaluate the extent to which the observation errors contaminate the forecast.

The equations of motion in the preforecast integration in this study can simply be written

$$\frac{\partial}{\partial t}\mathbf{V}_k = F(\mathbf{X},t) + \lambda(\mathbf{V}_k^0 - \mathbf{V}_k), \quad (2)$$

where k denotes the layer in the model where observations are available. Three different values for λ are tested: $\lambda_w = 10^{-4}$ s^{-1} for weak relaxation, $\lambda_s = 10^{-3}$ s^{-1} for strong relaxation, and $\lambda_a = \lambda_s(\delta t - t)/12$, -12 h $\leq \delta t \leq 0$ for attenuating relaxation. Fig. 2 illustrates the time variations of λ. Observations are assumed to be taken at 0 h and are assimilated into model prediction during -12 to 0 h in all of the assimilation experiments (Exps. 4–9).

5. Standard forecasts

During the period between -12 and 24 h, observation shows a rapid intensification of the tropical cyclone, the minimum central pressure deepens from

Unauthenticated | Downloaded 06/24/24 04:14 AM UTC

998 to 953 mb (Fig. 3), and the maximum wind speed increases from 29 to 52 m s^{-1} (Fig. 4). A 36 h forecast starting from −12 h (Exp. 2) and a 24 h forecast starting from 0 h (Exp. 3) are conducted based on the error-free initial mass field and nondivergent, gradient-balanced wind fields. Typical wind speed errors in the initial wind field are illustrated in Fig. 1.

As expected from previous experience, both forecasts have an initial dissipation stage due to the onset of the surface friction. The weakening of storm intensity is especially pronounced in Exp. 3 in that it has larger intensity errors before 12 h than Exp. 2 which is initialized 12 h earlier. This is indicative of the inadequacy of the static, nondivergent initialization employed. Improvement of forecast during the initial hours can be achieved by using a divergent static (Tarbell *et al.*, 1981) or a dynamical (Hovermale and Livezey, 1977; Kurihara and Bender, 1979) initialization scheme.

After the radial circulations develop, both forecasts reproduce the observed intensification but at slower rates. After 12 h, the 24 h forecast (Exp. 3) yields better prediction than the 36 h forecast by ~2 mb in minimum pressure and 2 m s^{-1} in maximum wind speed. Both forecasts predict weaker storm intensity as compared to the observation. The difference between the observed and predicted intensities at 24 h is about 15 mb in minimum pressure and 10 m s^{-1} in maximum wind speed. The divergence of the forecasts from the observation is a consequence of the "imperfect" physical parameterizations in the forecast model.

We selected the rms errors ($\bar{e}$) as a measurement of the accuracy of the predictions (Panofsky and Brier, 1968). Evolutions of $\bar{e}$ for wind speed (V), temperature (T) and specific humidity (q) with respect to the observation for Exps. 2 and 3 are shown in Figs. 5, 6 and 7, respectively. The initial $\bar{e}(V)$ is large at about 4 m s^{-1} in both experiments due to the non-divergent initialization. It decreases for the first 18 h in both experiments as the forecast storms intensify. As evident in Exp. 2 after 6 h, values of $\bar{e}(V)$ begins to increase, indicating a deteriorating forecast.

Both $\bar{e}(T)$ and $\bar{e}(q)$ increase rapidly after initialization with time from the error-free mass field. Their values escalate to 1.5 K in temperature and ~0.9–1.1 g kg^{-1} in specific humidity at 24 h. Here again, Exp. 3 produces a better prediction than Exp. 2 during most of the period 0–24 h.

6. Forecasts with assimilation of low-level winds

In Exps. 4, 5 and 6, the observed low-level radial (u_6) and tangential (v_6) winds at 0 h are assimilated by DIR into the 24 h forecast during a preforecast integration from −12 to 0 h (Table 2). The relaxation coefficients are λ_w, λ_s and λ_a in Exps. 4, 5 and 6, respectively (Fig. 2).

Figs. 8 and 9 show the minimum pressures and the maximum wind speeds for these three forecasts with low-level winds assimilated. It is apparent that the DIR with the weak relaxation coefficient (Exp. 4) does not alter the prediction appreciably toward the

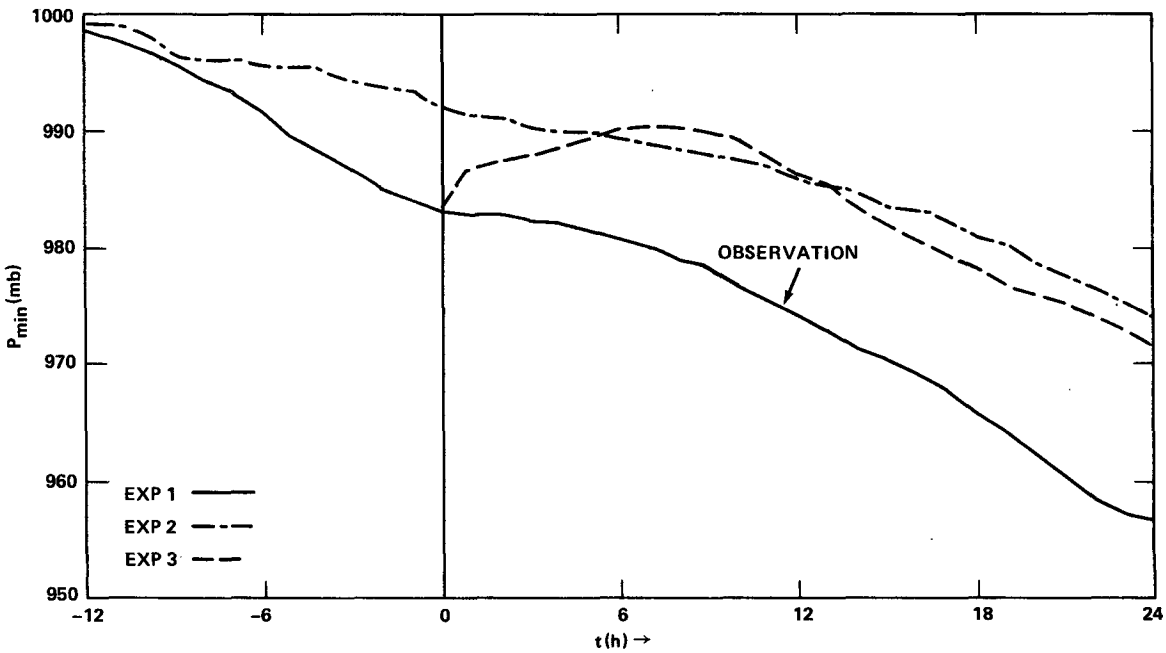

FIG. 3. The minimum pressures of the observation (Exp. 1) and standard forecasts (Exps. 2 and 3).

Unauthenticated | Downloaded 06/24/24 04:14 AM UTC

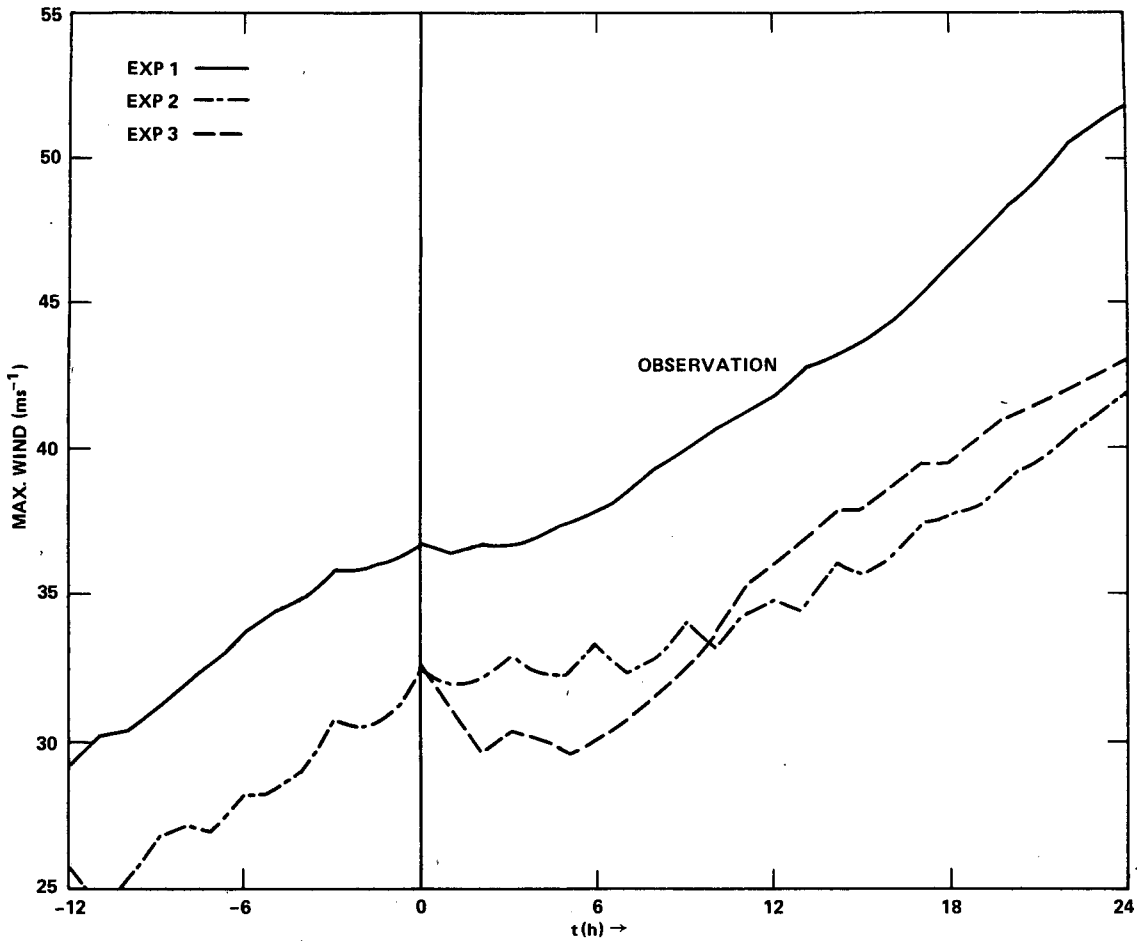

FIG. 4. The maximum wind speeds of the observation (Exp. 1) and standard forecasts (Exps. 2 and 3).

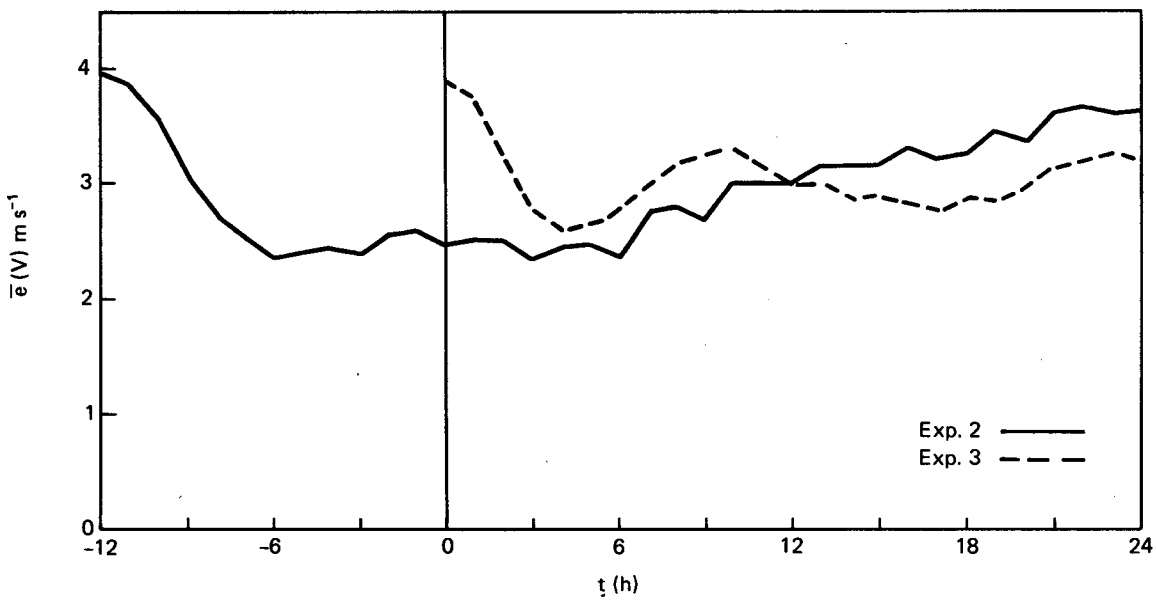

FIG. 5. The time series of the forecast rms errors in total winds for Exps. 2 and 3.

Unauthenticated | Downloaded 06/24/24 04:14 AM UTC

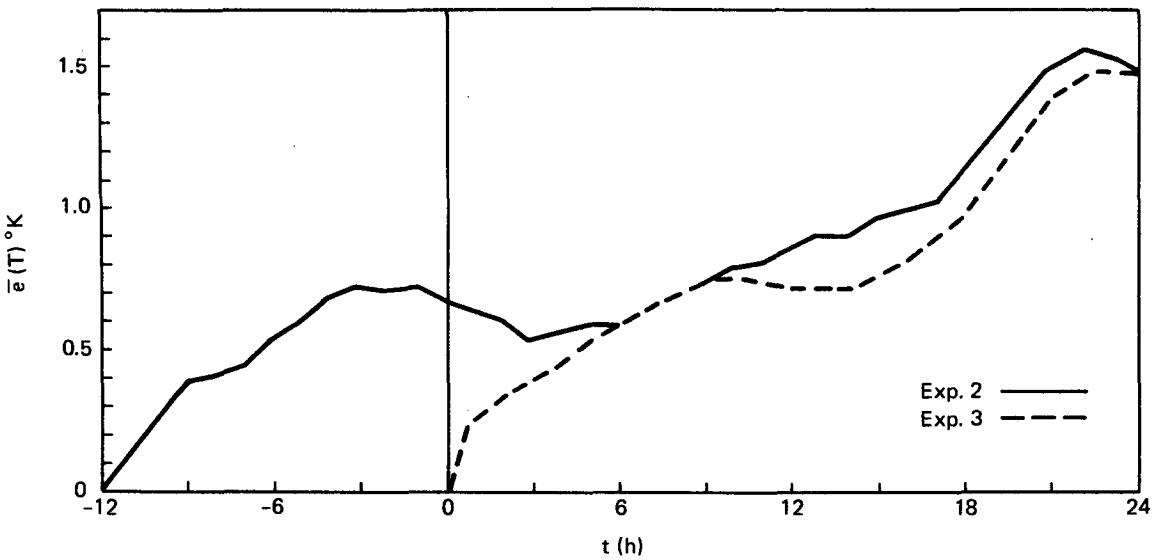

FIG. 6. The time series of the forecast rms errors in temperatures for Exps. 2 and 3.

observation during the preforecast integration. The following 24 h forecast shows no apparent improvement over the standard forecasts.

The model adjustments are considerable when strong and attenuating relaxation coefficients are applied in Exps. 5 and 6. The maximum wind speed in the preforecast integration converges to the observed value at 0 h within 6 h, in agreement with the theory of geostrophic adjustment. The maximum wind speed in Exp. 5 achieves the observed value

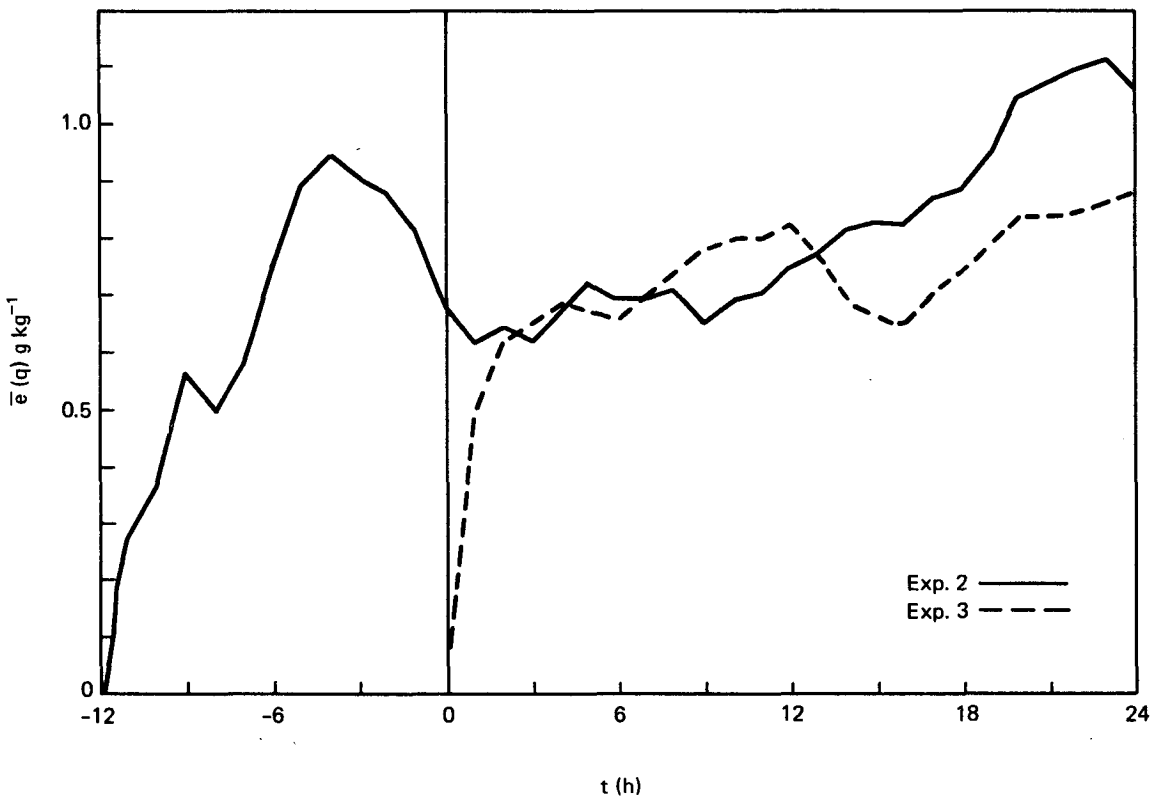

FIG. 7. The time series of the forecast rms errors in specific humidity for Exps. 2 and 3.

Unauthenticated | Downloaded 06/24/24 04:14 AM UTC

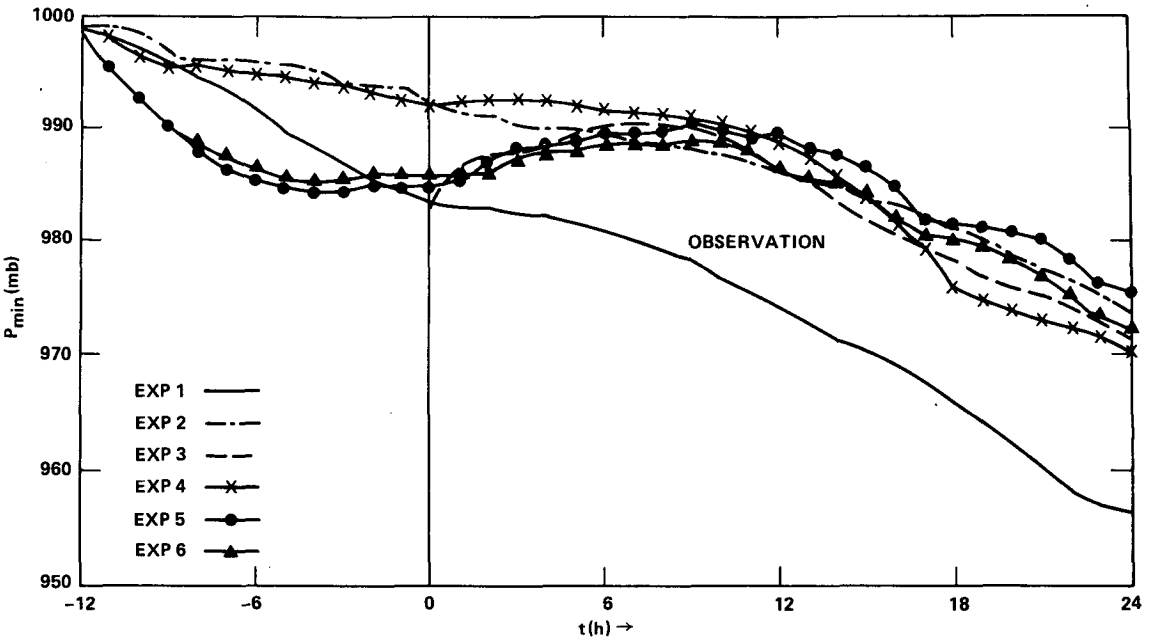

FIG. 8. As in Fig. 3 except for Exps. 4, 5 and 6.

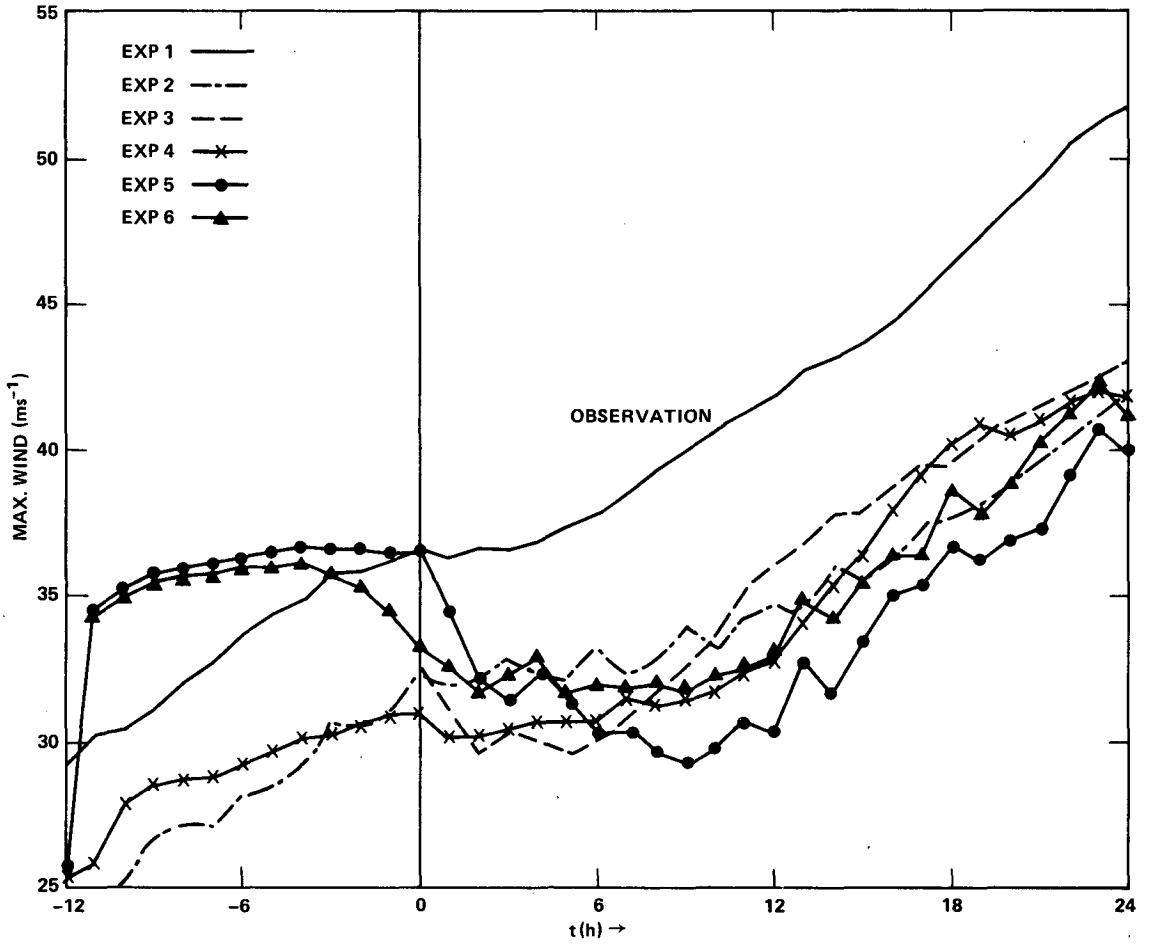

FIG. 9. As in Fig. 4 except for Exps. 4, 5 and 6.

Unauthenticated | Downloaded 06/24/24 04:14 AM UTC

due to constantly strong relaxation. However, as the assimilation terminates at 0 h, strong model adjustments occur in both experiments. The model rejection occurs in Exp. 5 where the maximum wind speed decreases approximately 5 m s^{-1} in 3 h and stays lower than that of the standard forecast (Exp. 2). The adjustment is milder in Exp. 6, but there is still no improvement in intensity forecast.

We thus conclude that low-level wind observations are not beneficial to intensity forecasts of tropical cyclones if assimilated by DIR. We can also conclude that the attenuating relaxation coefficient λ_a is more effective in assimilating the observed data (cf. Fig. 9) and desirable for eliminating model adjustments.

However, an examination of forecast errors in Exps. 4–6 is warranted. During the preforecast integration, $\bar{e}(V)$ decreases with time as relaxation forces the low-level wind to asymptotically approach the 0 h observation. The $\bar{e}(V)$ value from Exp. 5 at 0 h reaches the lowest level of all (Fig. 10). The model adjustments cause the error to be at levels higher than those of the standard forecasts (Exps. 2 and 3) after 6 h since the assimilation has been rejected by the model. The $\bar{e}(T)$ and $\bar{e}(q)$ are similar to $\bar{e}(V)$ in that they decrease with time in the preforecast integration for strong relaxation and they subsequently increase to levels equivalent or higher than those of the standard forecasts.

The rejection of assimilation of low-level winds in the preceding experiments can be attributed to the insufficient vertical coupling between the low-level and high-level momentum fields during the 12 h period of preforecast integration. A longer period of preforecast integration may produce enough vertical coupling through model dynamics and physics, but is not very meaningful in practice. It is then logical to test assimilation of additional wind observations at higher levels since they can be made available (Rodgers *et al.*, 1979).

7. Forecasts with assimilation of low- and higher-level winds

As listed in Table 2, observations of higher level winds in addition to the low-level winds are assimilated by DIR using relaxation coefficient λ_a. In Exp. 7, v_5 (check Table 1 for pressure level) at 0 h is assimilated; in Exp 8, v_4 and v_5; and in Exp. 9, u_2 and v_2.

The assimilations of higher level winds yield significantly different intensity forecasts from the standard forecasts as evident in Figs. 11 and 12 showing the minimum pressure and the maximum wind speed, respectively. In addition, the three experiments forecast very different minimum pressures even during the preforecast integration where the same λ_a is used. Among the three, Exp. 8 yields the best prediction, with maximum difference of only 4.5 mb in central pressure at 24 h. Exp. 7 predicts a very intense storm with central pressure deepening to 955 mb at 12 h. Although Exp. 9 predicts a weaker storm than the observation, it forecasts better than the standard forecasts (Exps. 2 and 3) and forecasts where only low-level winds are assimilated (Exps. 4, 5, and 6).

It is quite interesting that the storm intensities in Exps. 7 and 8 are drastically different when

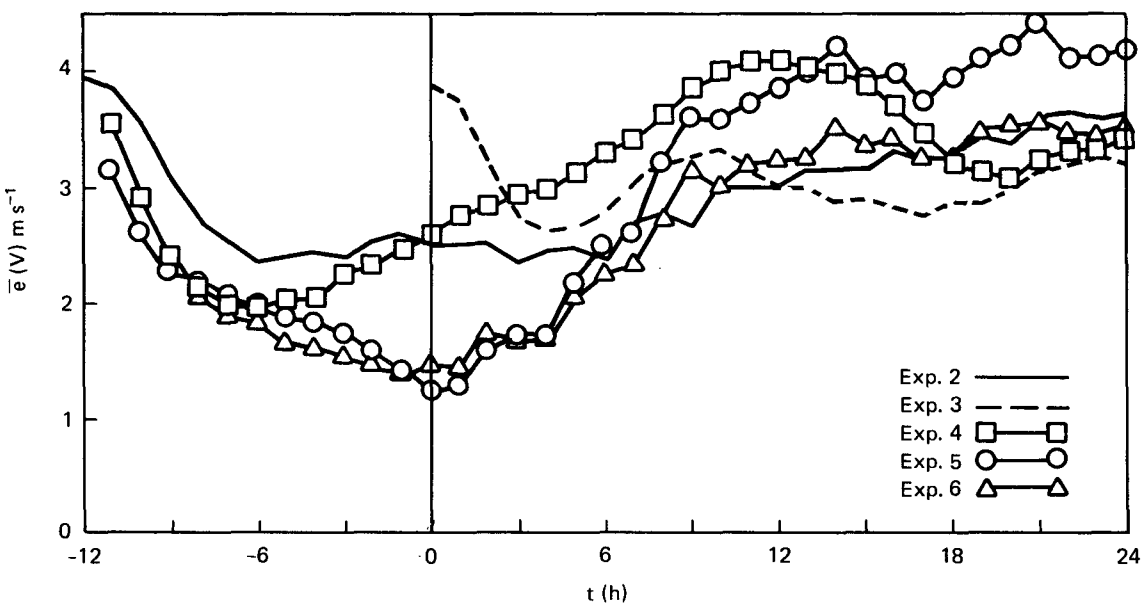

FIG. 10. As in Fig. 5 except for Exps. 4, 5 and 6.

Unauthenticated | Downloaded 06/24/24 04:14 AM UTC

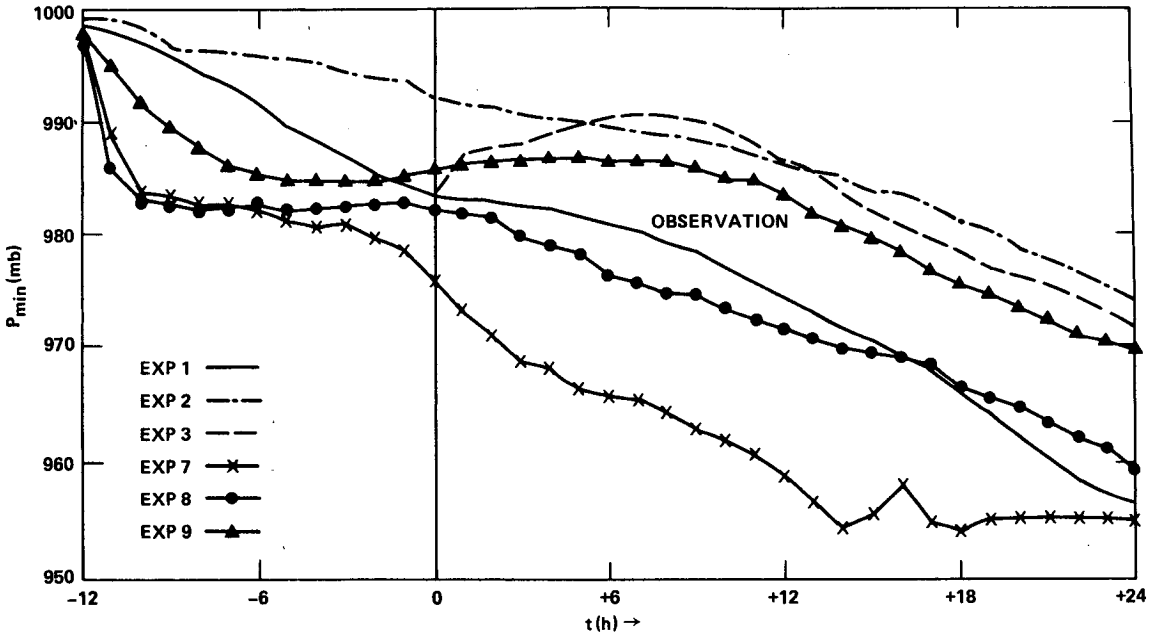

FIG. 11. As in Fig. 3 except for Exps. 7, 8 and 9.

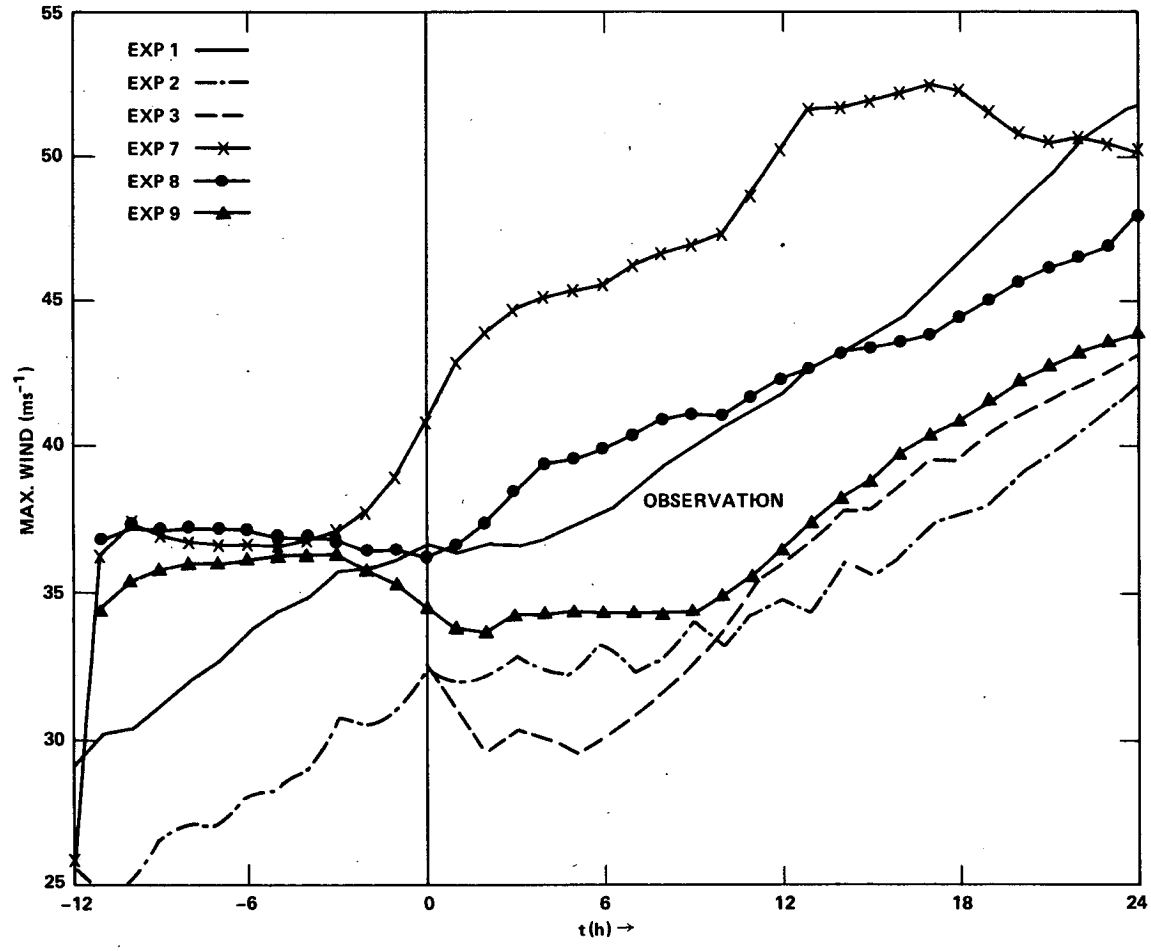

FIG. 12. As in Fig. 4 except for Exps. 7, 8 and 9.

Unauthenticated | Downloaded 06/24/24 04:14 AM UTC

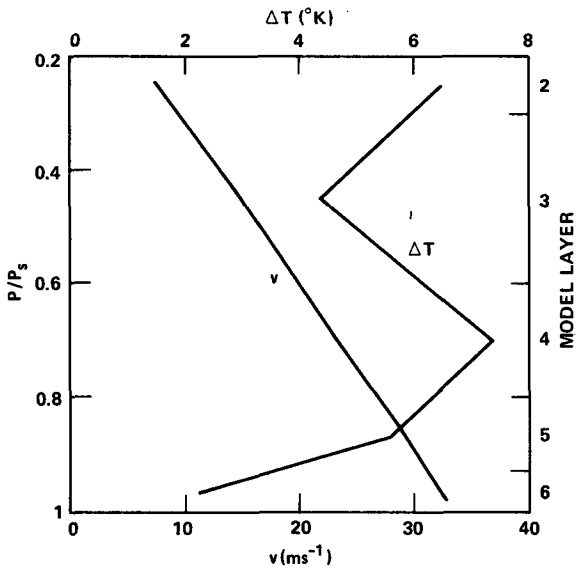

FIG. 13. The vertical profile of tangential velocity (v) showing the strong vertical shear, and the temperature anomalies (ΔT) showing the warm core at r = 30 km at 0 h of the observation.

the only difference in the experiments is that the observations of v_4 at 0 h are available for assimilation in Exp. 8. As demonstrated by the vertical profile of v at r = 30 km in Fig. 13, there is a strong vertical shear in the 0 h tangential wind observation. Tangential wind speed decreased upward associated with the strong warm core at level 4. In Exp. 7, the too strong storm intensity is due to the assimilation of the stronger circulation below 800 mb, whereas the vertically decreasing tangential circulation and effects of warm core are properly assimilated in Exp. 8. This suggests that when observational data are to be vertically interpolated in diagnosis or analysis, strong vertical shear and the related baroclinic effect must be taken into account.

The forecast errors in wind speed, temperature and water vapor are shown in Figs. 14, 15 and 16, respectively. The values of $\bar{e}(V)$ decrease in time during the preforecast integration as in Exps. 4, 5 and 6. Note the $\bar{e}(V)$ in Exp. 9 is the smallest because initial errors are largest at the assimilated levels (Fig. 1). The errors in Exps. 8 and 9 remain smaller than those of the standard forecasts, especially in Exp. 8, where the error is 50% lower.

The error in temperature field of Exp. 7 arises early in the preforecast integration. This shows that the effects of the warm core on tangential circulation are not properly assimilated as mentioned earlier. The errors in Exps. 8 and 9 are generally smaller than for the standard forecasts throughout the 24 h forecast period. The specific humidity errors for these three forecast experiments are higher than for the standard forecasts with Exp. 7 having the highest error. Between −12 and 6 h, $\bar{e}(q)$ in Exp. 8 is very low because the inflow and outflow, which nearly determine the net total water vapor convergence, are assimilated.

The higher $\bar{e}(q)$ in Exps. 8 and 9, in spite of the better intensity forecasts and lower $\bar{e}(V)$ and $\bar{e}(T)$, is probably due to the different physical parameterizations in the forecast model.

8. Deterioration of forecast due to satellite observation errors

In previous sections, we have examined the impact of assimilating the error-free satellite winds. The as-

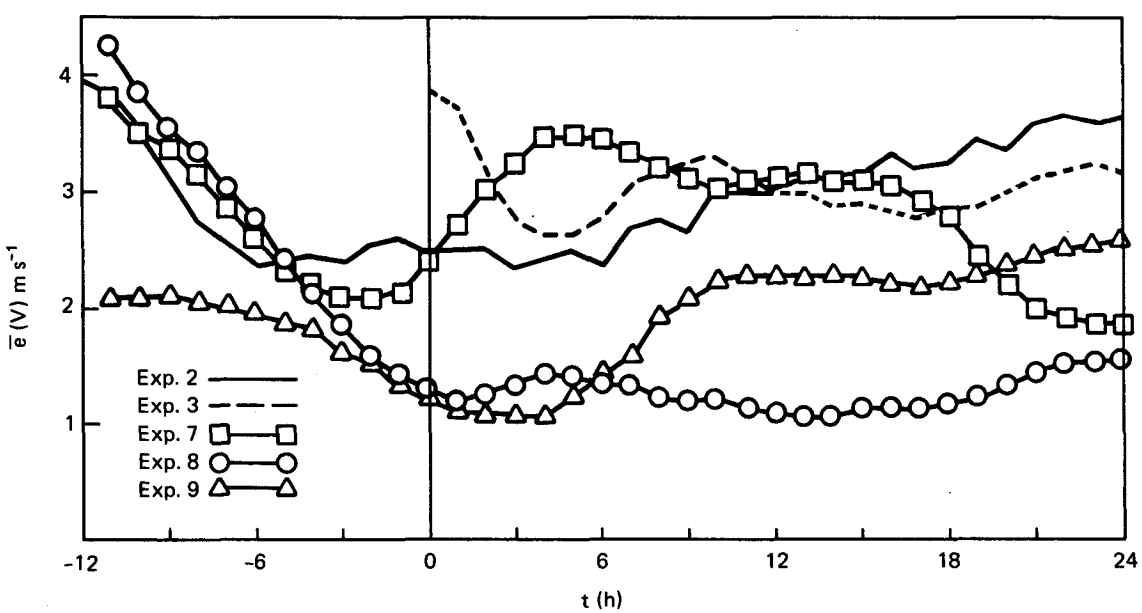

FIG. 14. As in Fig. 5 except for Exps. 7, 8 and 9.

Unauthenticated | Downloaded 06/24/24 04:14 AM UTC

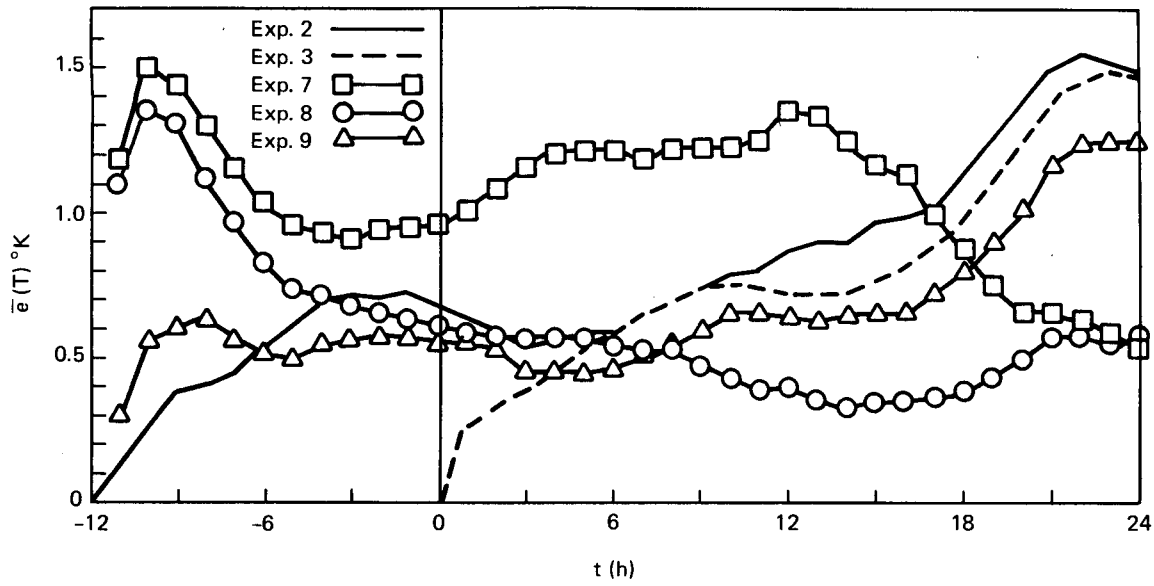

FIG. 15. As in Fig. 6 except for Exps. 7, 8 and 9.

sumption of perfect satellite observation is for clarity in comparison. Satellite-sensed winds are, of course, not error-free. As discussed earlier, the mean speed error in satellite winds varies from 2.5 m s^{-1} (Rodgers *et al.*, 1979) to as large as 8 m s^{-1} (Black, 1979). We now turn our attention to the influence of the satellite observation errors on the forecast.

Because winds at low and outflow level are most likely to be obtainable operationally, we repeat Exp. 9 with artificially introduced observation errors in both the initial condition and satellite-sensed winds. Randomized error of ~2.5 m s^{-1} and biased errors are added into the observation at −12 h. The biased errors have a maximum of 8 m s^{-1} at r = 30 km, decreasing with radius to zero at r = 150 km. These errors, after the balanced static initializations, are equivalent to approximately 0.5 K errors in the temperature field and a 4 mb error in central pressure. Four experiments (Exps. 2E, 3E, 9E and 9E2) are carried out based on initial conditions containing such errors. The satellite-sensed winds at 0 h contain random errors with maximum speed error of 2.5 m s^{-1} in Exp. 9E and 5 m s^{-1} in Exp. 9E2. Exps. 2E and 3E are identical to Exps. 2 and 3 except for the introduced errors in the initial condition.

As summarized in Table 3, the average 12 and 24 h forecasts in Exps. 2E, 3E and 9E are worse than their respective counterparts in error-free simulations. For example, Exp. 9 has an averaged forecast error of 11 mb in minimum pressure, 6.5 m s^{-1} in maximum wind speed and 2.5 m s^{-1} in $\bar{e}(V)$, whereas Exp. 9E has an averaged forecast error of 16 mb, 11.7 m s^{-1} and 4.5 m s^{-1}. It is encouraging that Exp. 9E, in which the magnitude of the observation errors are typical for operational forecasts, is a better forecast than the standard forecasts of Exps. 2E and 3E. It forecasts better than the standard forecasts by 4 mb in minimum pressure, approximately 2 m s^{-1} in maximum wind, and 0.5 in $\bar{e}(V)$. It is also interesting that Exp. 9E2 performs only slightly worse than Exp. 9E, although the error level is twice as large as that in Exp. 9E.

From the above comparison, we conclude that the errors in satellite winds could deteriorate a forecast, and that the assimilation of satellite low-level and outflow-level winds can improve the forecast if these errors are less or equal to those contained in the initial wind field.

9. Summary and discussion

The impact of accurately measured marine surface winds of sufficient spatial coverage and resolution in the 24 h intensity forecast of tropical cyclones has been studied with simulation experiments. The model physics in the forecast model were altered from those in the nature model. The observations are assimilated into the numerical forecast with dynamical initialization by relaxation during the preforecast integrations from error-free mass fields.

The results indicate no improvement in forecast accuracy when low-level winds are assimilated according to the abovementioned procedure. We note that a strong relaxation coefficient causes rejection of the assimilation within a few hours of forecasting and that a weak relaxation coefficient is ineffective.

Significant improvements are achieved when all winds below 600 mb are assimilated. This conclusion is easily understandable because the major characteristics of the tropical cyclone such as the vortex

Unauthenticated | Downloaded 06/24/24 04:14 AM UTC

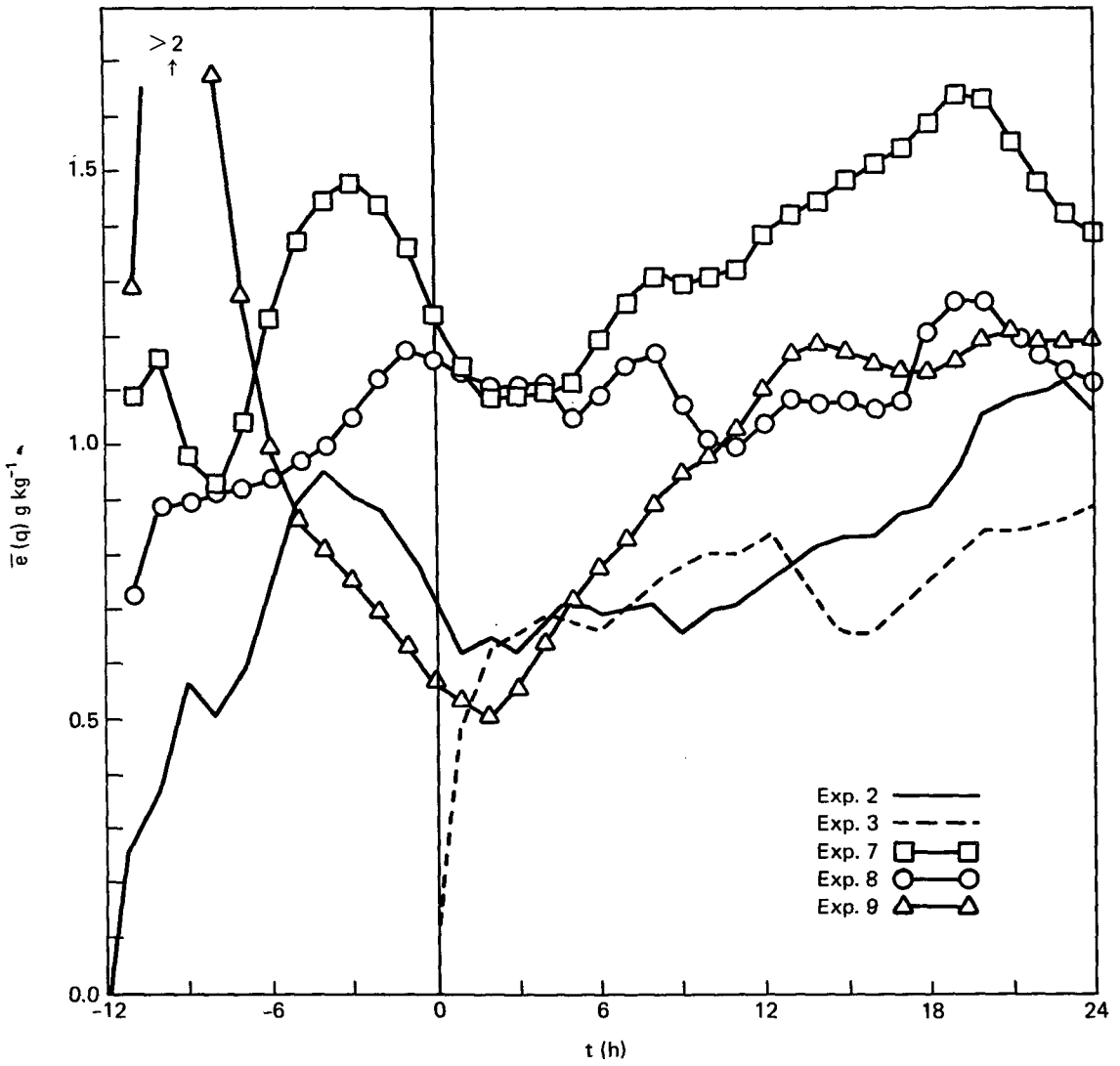

FIG. 16. As in Fig. 7 except for Exps. 7, 8 and 9.

strength, the warm core and the vertical shear are included in such observations. But simultaneous, high-resolution observations required for such assimilation are difficult to obtain. It is encouraging that forecast improvement can also be achieved when winds of low and outflow levels are assimilated because wind fields at these two levels are most likely available from satellite observations.

TABLE 3. 12 and 24 h averaged forecast errors.

Experiment	Initial $\bar{e}(V)$ (m s^{-1})	Magnitude of satellite observation error (m s^{-1})	12 and 24 h forecast errors			
			Min P (mb)	Max wind (m s^{-1})	$\bar{e}(V)$ (m s^{-1})	$\bar{e}(T)$ (K)
2	~4	—	15	8.5	3.2	1.18
3	~4	—	13	7.2	3.1	1.09
9	~4	0	11	6.5	2.5	0.95
2E	~5	—	21	13.4	5.0	1.75
3E	~5	—	20	13.1	4.9	1.67
9E	~5	2.5	16	11.7	4.5	1.5
9E2	~5	5	17	11.8	4.6	1.5

Unauthenticated | Downloaded 06/24/24 04:14 AM UTC

The forecast in which winds at these levels are assimilated worsens with increasing observation errors. However, even if the rms errors in the satellite observation are equivalent to those in the initial wind field, assimilation of low- and outflow-level winds still improves the forecast.

Caution must be taken in interpreting these findings for operational applications, as is the case for all simulation studies, because the extent to which they approximate reality is difficult to determine. The finding that the low-level wind observations alone cannot improve the forecast when assimilated by DIR should not cast doubt on the usefulness of observing systems which measure marine surface winds. Since an axisymmetric tropical cyclone is employed in this study, the position of the storm is assumed known. Also, the mass fields are assumed to be error-free in the static initializations of the forecasts. The precise center location and perfect mass field are not commonly available for operational forecasts, where meteorologists have to be content with uncertainties of the storm center position and with the "bogussed" circulations. The marine surface winds are invaluable in defining the low-level circulations and in locating the storm centers which otherwise would be impossible over data-void oceans.

Since our results with assimilation of the low-level and outflow-level winds are encouraging and since these will be the focal levels in satellite observations, future research with a three-dimensional tropical cyclone model is warranted. In a three-dimensional study, the impact of the satellite-sensed winds on storm track forecasts can be investigated. The effects of time lag within one satellite revolution discussed earlier and the effects of the swath width can also be studied. Finally, real data case studies can be carried out with a three-dimensional model.

Acknowledgments. The author thanks Dr. Rangarao V. Madala for his interest and Mrs. Jane Polson for typing the manuscript. Drs. W. Chao, D. F. Strobel, M. R. Schoeberl and R. T. Williams commented on the manuscript.

The research is supported by the Naval Research Laboratory through Contract N00173-80-C-0252.

REFERENCES

Anthes, R. A., 1974: Data assimilation and initialization of hurricane prediction models. *J. Atmos. Sci.*, **31**, 702–719.

Anthes, R. A., 1977: A cumulus parameterization scheme utilizing a one-dimensional cloud model. *Mon. Wea. Rev.*, **105**, 270–286.

——, and S. W. Chang, 1978: Response of the hurricane boundary layer to changes of sea-surface temperature in a numerical model. *J. Atmos. Sci.*, **35**, 1240–1255.

Bengtsson, L., 1975: Four-dimensional assimilation of meteorological observations. GARP Publ. Ser. No. 15, WMO, 76 pp.

Black, P. G., 1979: SEASAT-derived surface wind fields in eastern Pacific Hurricane FICO. *12th Tech. Conf. Hurricane and Tropical Meteorology, Bull. Amer. Meteor. Soc.*, **59**, 1356 (Abstract).

Brown, J. A., Jr., and K. A. Campana, 1978: An economical time-differencing system for numerical weather prediction. *Mon. Wea. Rev.*, **106**, 1125–1136.

Cane, M. A., V. J. Cardone, M. Halem, I. Halberstram and J. Ulrich, 1979: Observing systems simulation and potential impact of marine surface wind data on numerical weather prediction. Submitted to *Mon. Wea. Rev.*

Cardone, V. J., J. D. Young, W. J. Pierson, R. K. Moore, J. A. Greenwood, C. Greenwood, A. K. Fung, A. Salfi, H. L. Chan, M. Afarani and M. Komen, 1976: The measurement of the winds near the ocean surface with a radiometer-scatterometer on Skylab. A joint meteorological, oceanographic, and sensor evaluation program for Experiment S193 on Skylab. NASA CR-147478.

Chang, S. W., 1977: The mutual response of the tropical cyclone and the ocean as revealed by an interacting atmospheric and oceanic model. Ph.D. dissertation, Pennsylvania State University, 210 pp.

——, 1981: Test of a planetary boundary layer parameterization based on generalized similarity theory in tropical cyclone models. *Mon. Wea. Rev.* (in press).

Charney, J., M. Halem, and R. Jastrow, 1969: Use of incomplete historical data to infer the present state of the atmosphere. *J. Atmos. Sci.*, **26**, 1160–1163.

Davies, H. C., and R. E. Turner, 1977: Updating prediction models by dynamic relaxation: An examination of the technique. *Quart. J. Roy. Meteor. Soc.*, **103**, 225–245.

Elsberry, R. L., 1977: Operational data tests with a tropical cyclone model. Tech. Rep. NPS-63ES 77031, Naval Postgraduate School, 28 pp.

Ghil, M., M. Halem and R. Atlas, 1979: Time-continuous assimilation of remote-sounding data and its effect on weather forecasting. *Mon. Wea. Rev.*, **107**, 140–171.

Hoke, J. E., and R. A. Anthes, 1976: The initialization of numerical models by a dynamic-initialization technique. *Mon. Wea. Rev.*, **104**, 1551–1556.

——, and R. A. Anthes, 1977: Dynamic initialization of a three-dimensional primitive-equation model of Hurricane Alma of 1962. *Mon. Wea. Rev.*, **105**, 1211–1350.

Hovermale, J. B., and R. E. Livezey, 1977: Three-year performance characteristics of the NMC hurricane model. *Preprints 11th Tech. Conf. Hurricane and Tropical Meteorology*, Miami Beach, Amer. Meteor. Soc., 122–125.

Jones, W. L., and W. J. Pierson, 1978: Preliminary evaluation of scatterometer winds from SEASAT-A. Paper presented at American Geophysical Union meeting, San Francisco.

Kasahara, A., and D. Williamson, 1972: Evaluation of tropical wind and reference pressure measurements: Numerical experiments for observing systems. *Tellus*, **24**, 100–115.

Kuo, H. L., 1974: Further studies of the parameterization of the influence of cumulus convection on large-scale flow. *J. Atmos. Sci.*, **31**, 1232–1240.

Kurihara, Y., and M. A. Bender, 1979: Supplementary note on "A scheme of dynamic initialization of the boundary layer in a primitive equation model." *Mon. Wea. Rev.*, **107**, 1219–1221.

McPherson, R. D., 1975: Progress, problems, and prospects in meteorological data assimilation. *Bull. Amer. Meteor. Soc.*, **56**, 1154–1166.

Monin, A., and A. Obukhov, 1959: A note on the general classification of motions in a baroclinic atmosphere. *Tellus*, **11**, 159–162.

Unauthenticated | Downloaded 06/24/24 04:14 AM UTC

Morel, P., and O. Talagrand, 1974: Dynamic approach to meteorological data assimilation. *Tellus*, **26**, 334–343.

Nitta, T., and J. B. Hovermale, 1969: A technique of objective analysis and initialization for the primitive forecast equations. *Mon. Wea. Rev.*, **97**, 652–658.

Panofsky, H. A., and G. W. Brier, 1968: *Some Applications of Statistics to Meteorology*. The Pennsylvania State University Press (see p. 200).

Rodgers, E., R. C. Gentry, W. Shenk, and V. Oliver, 1979: The benefits of using satellite short-interval satellite images to derive winds for tropical cyclones. *Mon. Wea. Rev.*, **107**, 575–584.

Sasaki, Y., 1969: Proposed inclusion of time variation terms, observational and theoretical, in numerical variational objective analysis. *J. Meteor. Soc. Japan*, **47**, 115–124.

Sheets, R. C., 1969: Some mean hurricane soundings. *J. Appl. Meteor.*, **8**, 134–146.

Tarbell, T. C., T. T. Warner and R. A. Anthes, 1981: An example of the initialization of the divergent wind component in a mesoscale numerical weather prediction model. *Mon. Wea. Rev.*, **109**, 77–95.

Washington, W., 1964: A note on the adjustment towards geostrophic equilibrium in a simple fluid system. *Tellus*, **16**, 530–534.

——, and A. Kasahara, 1971: Adaptation of meteorological variables forced by updating. *J. Atmos. Sci.*, **28**, 1313–1324.

Yamada, T., 1976: On the similarity functions A, B and C of the planetary boundary layer. *J. Atmos. Sci.*, **33**, 781–793.

Yu, T.-W., 1980: A marine boundary layer wind analysis scheme for atmospheric circulation models. *Third Conf. Ocean-Atmosphere Interaction, Bull. Amer. Meteor. Soc.*, **60**, 1255 (Abstract).

Williamson, D., 1973: The effect of forecast error accumulation on four-dimensional data assimilation. *J. Atmos. Sci.*, **30**, 537–543.

Unauthenticated | Downloaded 06/24/24 04:14 AM UTC